J Fluoresc (2009) 19:511–516
DOI 10.1007/s10895-008-0440-0

ORIGINAL PAPER

Er-Yb Codoped Ferroelectrics for Controlling Visible Upconversion Emissions

Tung-Ching Huang · Wen-Feng Hsieh

Received: 25 July 2008 / Accepted: 3 November 2008 / Published online: 5 December 2008

Abstract Under a 980 nm laser pumping, quenching of green upconversion (UC) emission accompanied with enhancement of red UC emission observed was dominated by the energy back-transfer (EBT) process in Er^{3+} and Yb^{3+} co-doped $PbTiO_3$, $BaTiO_3$, and $SrTiO_3$ polycrystalline powders. The efficiency of the EBT process depends not only on Yb^{3+} concentration but also on level match of the doped Er^{3+} and Yb^{3+} ions caused by the crystal fields with different symmetries. Our UC emission spectra and X-ray diffraction confirm that the centrosymmetric crystal field arising from reducing tetragonality causes level match of transition $^4S_{3/2} \rightarrow {}^4I_{13/2}$ of Er^{3+} and $^2F_{7/2} \rightarrow {}^2F_{5/2}$ of Yb^{3+}. This level match is responsible for enhancing red UC emission.

Keywords Upconversion · Fluorescence · Rare-earth · X-ray diffraction · Crystal structure

Introduction

Upconversion (UC) in rare-earth (RE) ion-doped materials has been intensively studied in recent years of applications in laser devices [1, 2], three-dimensional display [3], sensors [4], and biological fluorescent labels [5–7]. Energy UC of radiation can exist by intra-ionic successive absorption, cooperative energy transfer, and photon avalanche processes [8, 9]. The research of these mechanisms provides intellects on the physics of energy transfer processes and fluorescence converters. Recently, green and red UC radiation induced by a 980-nm diode laser excitation in Er^{3+}-doped and Er^{3+}—Yb^{3+} co-doped Y_2O_3 and ZrO_2 nanocrystals were reported [10–12]. It is known that the Er^{3+} ion absorbs one laser photon and jumps from the ground state $^4I_{15/2}$ to the long-lived $^4I_{11/2}$ state, which is termed the ground-state absorption (GSA). Then, the excited-state absorption (ESA) could happen to populate $^4F_{7/2}$ state. Subsequently, the Er^{3+} ions at $^4F_{7/2}$ state could further rapidly relax to the $^2H_{11/2}/{}^4S_{3/2}$ state by multiphonon processes, from which the green UC emission arises. Thus, the green UC emission is a result of two-photon excitation (GSA followed by ESA) process. The codoped Yb^{3+} ions provide excitation of the $^4I_{11/2}(Er^{3+})$ state by the larger absorption cross section of Yb^{3+} ions.

The strong red UC emission is reported enabled by quenching the $^4S_{3/2}(Er^{3+})$ state to the saturation of the $^4I_{13/2}(Er^{3+})$ state through the so-called efficient energy back-transfer (EBT) process. [12] Through the exciting the nearest-neighboring Yb^{3+} ion at the ground state $^2F_{7/2}$ (Yb^{3+}) to the $^2F_{5/2}(Yb^{3+})$ state, the excited Er^{3+} ion located at the $^4S_{3/2}(Er^{3+})$ state, which originally emits green UC radiation, will transit to the $^4I_{13/2}(Er^{3+})$ state. This excitation was expressed as: $^4S_{3/2}\left(Er^{3+}\right) + {}^2F_{7/2}(Yb^{3+}) \rightarrow {}^4I_{13/2}\left(Er^{3+}\right) + {}^2F_{5/2}\left(Yb^{3+}\right)$ and the energy diagram schematically presented in Fig. 4 of Ref. 12 was duplicated in Fig. 1 for making explanation clearer. Chen, *et al.* [12] reported that the energy mismatch in the EBT process is about 320 cm^{-1} and can be easily dissipated by one phonon of the ZrO_2 lattice (470 cm^{-1}). The excited $^2F_{5/2}$–Yb^{3+} ions can be further dissipated by another excitation that the Er^{3+} ions transited from the ground state to the $^4I_{11/12}(Er^{3+})$ state then further relaxed to the long-lived $^4I_{13/2}(Er^{3+})$ state by the EBT process. The higher Yb^{3+} ion concentration could provide the more Yb^{3+} ions nearly neighboring to the Er^{3+} ions to cause the efficient EBT process. The $^4I_{13/2}$–Er^{3+} ion

T.-C. Huang · W.-F. Hsieh (✉)
Department of Photonics and Institute of Electro-Optical Engineering, National Chiao Tung University,
1001 Tahsueh Rd.,
Hsinchu 30050, Taiwan
e-mail: wfhsieh@mail.nctu.edu.tw

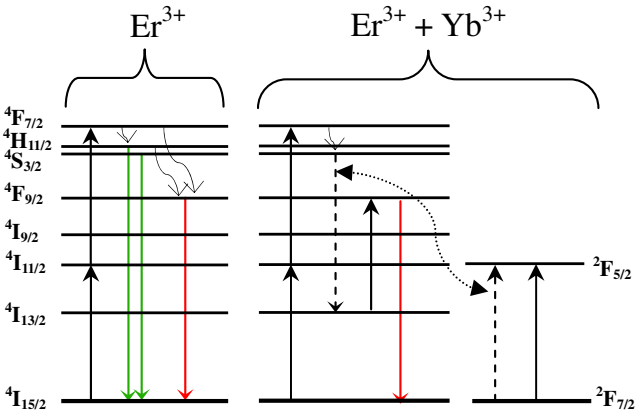

Fig. 1 Energy level diagram of Er^{3+} and Yb^{3+} ions as well as the proposed mechanisms to produce UC spectra

subsequently absorbs a laser photon from the $^4I_{13/2}$–(Er^{3+}) state or directly relaxes from the high-lying states to populate $^4F_{9/2}$–Er^{3+} state that the red UC emission arises. Thus, the efficient red UC radiation requires not only Yb^{3+} concentration but also level match of $^4S_{3/2} \rightarrow ^4I_{13/2}$ in Er^{3+} and $^2F_{7/2} \rightarrow ^2F_{5/2}$ in Yb^{3+} under assistance of phonon for efficient EBT process. Therefore, the red UC emission would be a mixing process of one-photon process [12] through the efficient EBT process and two-photon process through relaxing from the high-lying states after GSA and ESA.

However, the different crystal field caused by structure symmetry of the host materials would contribute to different perturbation terms for the Er^{3+} and Yb^{3+} inner shell transitions. Whether the energy match of level spacing $^4S_{3/2} \rightarrow ^4I_{13/2}$ of the Er^{3+} ion and $^2F_{7/2} \rightarrow ^2F_{5/2}$ of the Yb^{3+} ion or not should be sensitive not only to assistance of phonon but also to the crystal field resulting from symmetry of the crystal structure. Therefore, the crystal structure may be a more important mechanism for converting UC green radiation to red radiation due to the EBT process. In order to investigate the relationship between the crystal field and the match of energy levels, in this study, we chose $PbTiO_3$, $BaTiO_3$ and $SrTiO_3$ with different degrees of tetragonality as the host materials. Both $PbTiO_3$ and $BaTiO_3$ are ferroelectric perovskites which possess tetragonal phase at room temperature, while $SrTiO_3$ is a quantum paraelectric [13]. The tetragonality of $PbTiO_3$ ($c/a = 1.065$) is higher than that of $BaTiO_3$ ($c/a = 1.010$) according to the JCPDS-International Center for Diffraction Data No. 78-0298 and No. 83.1880.

Experimental details

Synthesis of powder samples

$PbTiO_3$, $BaTiO_3$, or $SrTiO_3$ powder samples simultaneously doped with 6 mol % Er^{3+} ions and 0 mol %, 6 mol %, and 12 mol % of Yb^{3+} ions, respectively, were synthesized according to a procedure described briefly as follows. Lead acetate (or barium acetate, strontium acetate), erbium acetate, and ytterbium acetate with corresponding mole ratio of cations were first sufficiently stirred for 20 min at 90°C for being completely dissolved in dehydrated acetic acid. Titanium isopropoxide was then added to the solution and kept stirring for another 20 min. We dried and solidified the solution under illumination of a 400 W infrared lamp for 36 hr. The resultant solid was ground into powders and then sintered at 700°C for 120 min in an Al_2O_3 crucible.

Characterization

The phases of powders were measured using a Mac science M18X X-ray diffractometer equipped with a rotating anode (Cu-$k\alpha$) line of wavelength 1.5405 Å. The emitted UC fluorescence spectra were performed at room temperature using a SPEX 1877C triple-grating spectrograph equipped with a liquid nitrogen-cooled CCD at 140 K. The excitation source was a 980 nm diode laser with maximal power output of 600 mW.

Results and discussion

UC fluorescence spectra

Figure 2 shows the UC fluorescence spectra of $PbTiO_3$ [Fig. 2a], $BaTiO_3$ [Fig. 2b] and $SrTiO_3$ [Fig. 2c] doped with 6 mol% Er^{3+} ions and various concentrations of Yb^{3+} ions under 980 nm excitation. As mentioned above and in the literature [12, 14], the emission bands around 550/565 nm (green) and 655/680 nm (red) originate from the intra 4*f*-4*f* electronic transitions $^2H_{11/2}/^4S_{3/2} \rightarrow ^4I_{15/2}$ and $^4F_{9/2} \rightarrow ^4I_{15/2}$ of the Er^{3+} ions, respectively. The green and red bands in this study are slightly shifted comparing to what appears in Ref. 12, we found the radiation peak positions and the spectral shapes of the red (around 665 nm) and the green fluorescent radiations (545/565 nm) are different from those in Ref. 12. It indicates that the different structure symmetry of host materials result in the different influence of crystal field on the energy levels of Er^{3+} and Yb^{3+}. The very weak red UC emission is a two-photon process at only Er^{3+} doping in various systems, which indicates a few population of $^4F_{9/2}$(Er^{3+}) state. The bandwidths of the two UC labels are found about 30 nm. In these spectra, besides the quenching of green UC emission with increasing Yb^{3+} concentration, which indicates decreasing the population of the $^2H_{11/2}/^4S_{3/2}$(Er^{3+}) state, we observed level splits in green UC emission of only Er^{3+} doping and co-doped 6 mol% Yb^{3+} ones in $PbTiO_3$ and $BaTiO_3$. It is attributed to the Stark splitting of the degenerate 4f levels under the strong

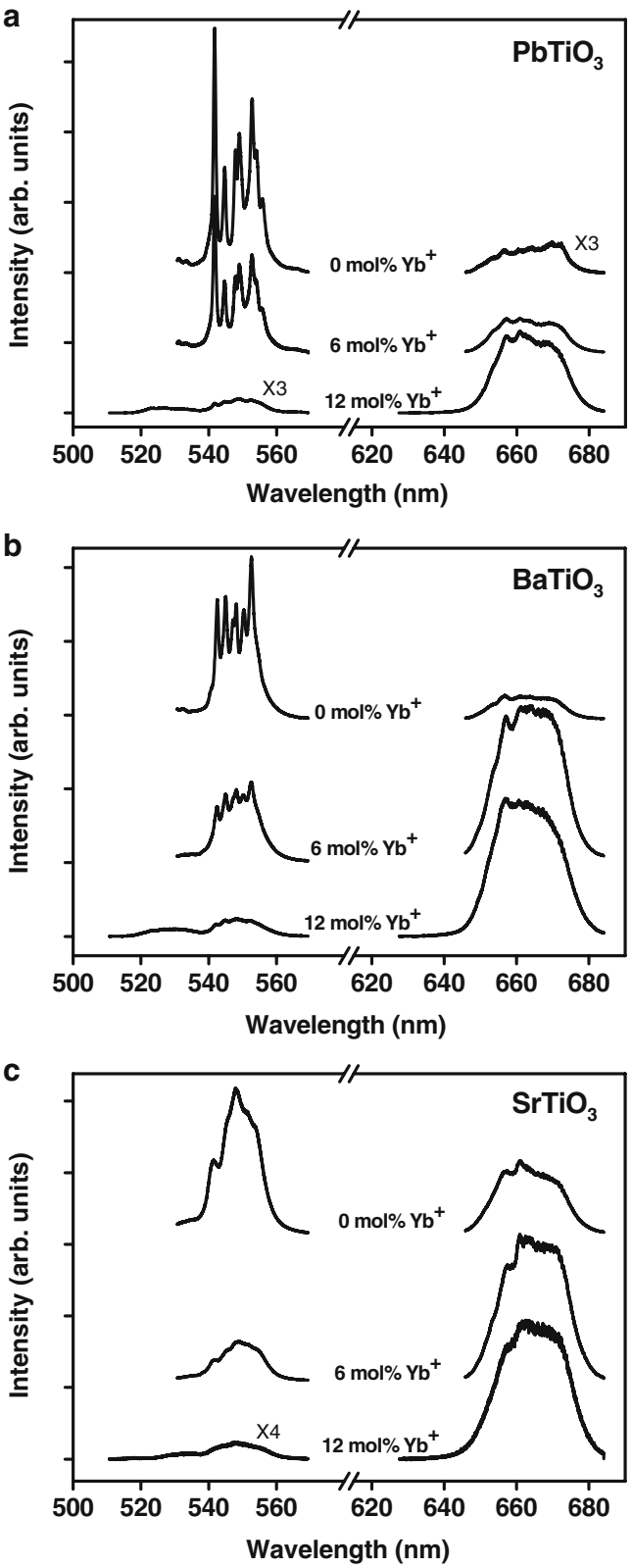

Fig. 2 UC fluorescence spectra of **a** $PbTiO_3$, **b** $BaTiO_3$, and **c** $SrTiO_3$ doped with 6 mol% Er^{3+} ions and various concentrations of Yb^{3+} ions under the same pump power of 980 nm diode laser at 107 mW

crystal field of the $PbTiO_3$ and $BaTiO_3$ [15–17]. The split in $PbTiO_3$ system is more obvious than that in $BaTiO_3$ system indicating the stronger influence of crystal field on the energy levels of Er^{3+} and Yb^{3+} in $PbTiO_3$ than in $BaTiO_3$ due to the larger asymmetric crystal field for the host material of larger tetragonality. On the other hand, the spectral shapes become smoother because of the weaker influence of the more centrosymmetric crystal field for high concentration Yb^{3+} (12 mol%) in both $PbTiO_3$ and $BaTiO_3$ systems and all samples in $SrTiO_3$ system. Fig. 2 also shows unobvious splits in all of the red UC emission spectra. It reveals that the underlying mechanism of the red UC emission differs from that of green one. The intensity of red UC emission greatly increases as the Yb^{3+}-ion concentration increases, that results from the increasing of the EBT process as reported by Chen, *et al*. [12]. The very weak red UC emission is a two-photon process at only Er^{3+} doping in various systems, which indicates a few population of $^4F_{9/2}(Er^{3+})$ state; whereas, the strong red UC emission and almost complete quenching of the UC green emission are observed at co-doped 12 mol% Yb^{3+}. The energy mismatch in the EBT process is about 320 cm^{-1} that can be easily dissipated by the aid of one phonon of the ZrO_2 lattice with energy 470 cm^{-1} in [12]. If the energy mismatch in the EBT process were dissipated by one phonon of the $PbTiO_3$ lattice with energy 290 cm^{-1} or 510 cm^{-1} and the $BaTiO_3$ lattice with 310 cm^{-1} or 520 cm^{-1}, then the intensity ratios of the green UC and the red UC should make no difference for the same amount of Yb^{3+} in $PbTiO_3$ and $BaTiO_3$. However, we observed that the red UC emission is stronger than the green one at co-doped 6 mol% Yb^{3+} in $BaTiO_3$ system, but weaker red UC emission in the $PbTiO_3$ system of the same doping. This reveals a weak EBT process in $PbTiO_3$ with 6 mol% Yb^{3+} co-doping. The observed spectral peak positions and shapes of green and red bands are slightly different from what observed in [12] that may be attributed to different crystal field. We observed a broad red emission around 665 nm with FWHM of 22 nm which is almost unchanged with crystal structure, but the position of maximal peak is at 544 nm (18,382cm^{-1}) at only Er^{3+} doping in $PbTiO_3$ while it changes to 555 nm (18,018 cm^{-1}) at the same doping in $BaTiO_3$. It indicates that the different structure symmetry of host materials resulted in the different influence of crystal field on the energy levels of Er^{3+} over a spectral range of 363 cm^{-1}. Therefore, the energy mismatch in the EBT process may be dissipated not only by the aid of phonons but also by Boltzmann distributed population within the manifold of $^4S_{3/2}$ or/and $^4I_{13/2}(Er^{3+})$ state affected by the crystal field with different symmetries. The strength of EBT process depends on whether the energy match of level space $^4S_{3/2} \rightarrow {}^4I_{13/2}$ of the Er^{3+} ion and $^2F_{7/2} \rightarrow {}^2F_{5/2}$ of the Yb^{3+} ion that strongly depends on crystal field due to

structure symmetry [14]. The match can be achieved for centrosymmetric media but may not be so due to the asymmetric crystal field in tetragonal phase, thus to lower the strength of EBT process. We will discuss the influence of change of the crystal structure on the EBT process in the following using x-ray diffraction.

Microstructure

Figure 3 displays the x-ray diffraction patterns of various concentrations of Er^{3+}- and Yb^{3+}- doped $PbTiO_3$ [Fig. 3a] and $BaTiO_3$ [Fig. 3b] with sintering temperature at 700°C. All the samples already show a tetragonal phase with various planes without obvious secondary phases, corresponding well to the standard powder diffraction pattern. To further investigate the variation of structures with the increase of Yb^{3+} concentration, a tetragonal single phase (*P4mm*) model was applied to refine the crystal structure with the XRD data.

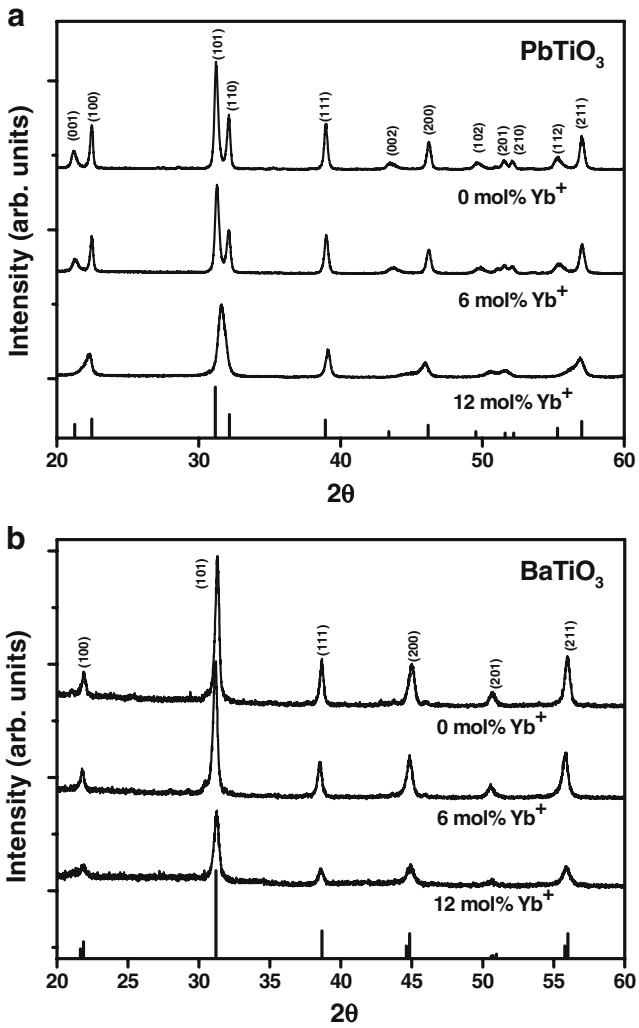

Fig. 3 XRD patterns of **a** $PbTiO_3$ and **b** $BaTiO_3$ doped with 6 mol% Er^{3+} ions and various concentrations of Yb^{3+} ions

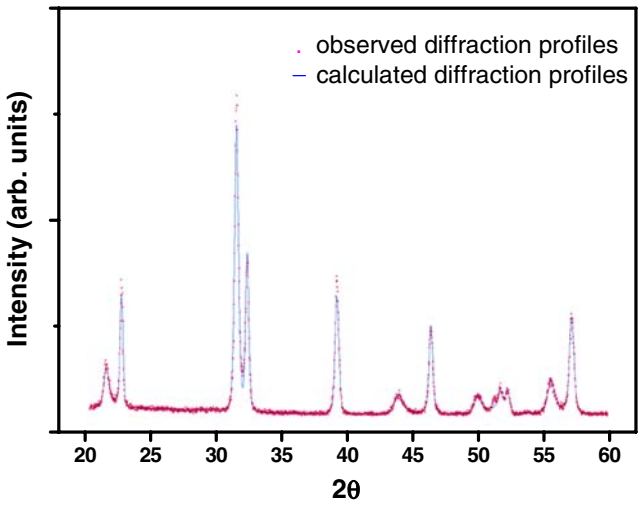

Fig. 4 Rietveld pattern of $PbTiO_3$ doped with only 6 mol% Er^{3+} ions and 6 mol% Yb^{3+} ions. Observed (*dot symbols*) and calculated (*solid curve*) X-ray intensity profiles

Here we just showed the refinement result of $PbTiO_3$ doped with 6 mol% Er^{3+} ions and 6 mol% Yb^{3+} ions in Fig. 4 and the calculated profiles agree well with the observed ones. Figure 5 plots the Yb^{3+} concentrations dependence of the tetragonality, *c*/*a*, and lattice constants following Rietveld refinement. As Yb^{3+}-ion concentration changes from 0, 6, to 12 mol %, the tetragonality (*c*/*a*) of $PbTiO_3$ system declines from 1.058, 1.053, to 1.020; moreover, *c*/*a* of $BaTiO_3$ system retains around 1.005. Decline of tetragonality is due to the presence of substitution of Er^{3+} and Yb^{3+} ions in $PbTiO_3$ that is similar to the results reported by Kuo *et al.* [18]. The declining tetragonality of $PbTiO_3$ system as increasing Yb^{3+} concentration will result in weakening the crystal field on Er^{3+} and Yb^{3+} ions, in turn, it benefits the match of the level space ${}^4S_{3/2} \rightarrow {}^4I_{13/2}$ of the Er^{3+} ion and ${}^2F_{7/2} \rightarrow {}^2F_{5/2}$ of the Yb^{3+} ion to enhance the EBT process. These results are consistent with the observed split of spectral peaks of green UC emission in tetragonal phase as well as the quenching of green UC emission and enhancement of red UC emission for high Yb^{3+} concentration with low tetragonality.

As compared with $PbTiO_3$ system and $BaTiO_3$ system at 6 mol% at Yb^{3+} concentration, the larger asymmetric crystal field for $PbTiO_3$ of larger tetragonality on Er^{3+} and Yb^{3+} ions results in the level mismatch. The weak strength of EBT process due to the larger asymmetric crystal field at 6 mol% at Yb^{3+} concentration in $PbTiO_3$ leads to weak red UC emission. It agrees with the result of the dependence of red UC emission on structure of host material at the same Yb^{3+} concentration.

Pump power

To verify the mechanism of red UC emission, we investigated the dependence of the intensity (I) of red UC emission on the

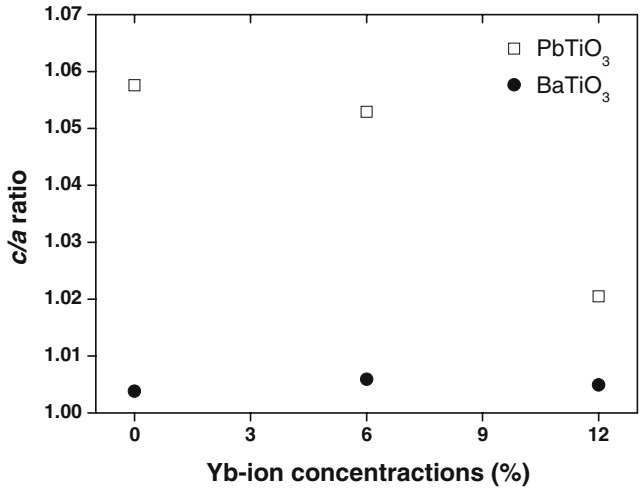

Fig. 5 *c/a* (*a* and *c* are lattice constants) ratio as function of Yb^{3+}- ion concentrations after Rietveld refinement

pump power (*P*). It is possible to determine the number of photons (*n*) required for populating the emitting state according to [19, 20]:

$$I \propto P^n. \quad (1)$$

Similar to Ref. [12], the *n* value is close to 2 for the green UC emission. Because we are more interested in the mechanism of red UC emission, we plotted the logarithm diagram of *I* versus *P* for both $PbTiO_3$ and $BaTiO_3$ systems in Fig. 6. As shown in Fig. 6a, the *n* value decreases from 1.58 for 0 mol % Yb^{3+}-ion to 1.47 for 6 mol % Yb^{3+}-ion concentration doped $PbTiO_3$, which indicate a mixing process of one- and two-photon for producing the red band with two-photon process being still the dominant mechanism. The EBT process is relatively weak because the strong crystal field due to the structure asymmetry contributes to the level mismatch between $^4S_{3/2} \rightarrow ^4I_{13/2}$ of Er^{3+} ion and $^2F_{7/2} \rightarrow ^2F_{5/2}$ of Yb^{3+} ion. However, for 12 mol% Yb^{3+} doping, the power law shows one-photon process dominant with $n = 1.22$, namely, the efficient EBT process takes over to effectively quench the $^4S_{3/2}$(Er) state and so to diminish the green band (see Fig. 2a) in the more centrosymmetric host matrices at the highest Yb^{3+}-ion concentration (Fig. 3a). On the contrary, the *n* value is also 1.55 in Fig. 6b for 0 mol% Yb^{3+} doped $BaTiO_3$, which is a two-photon process. It becomes 1.34 and 1.23 for Yb^{3+}-ion concentrations of 6 mol% and 12 mol%, respectively. Under this circumstance, the $^4S_{3/2}(Er^{3+})$ states, which the green UC radiation arises, were strongly quenched with low green emission in Fig. 2b via the EBT process to saturate the $^4I_{13/2}(Er^{3+})$ state through coupling with the transition $^2F_{7/2} \rightarrow ^2F_{5/2}$ of Yb^{3+} ion. And the strong red UC emission were observed dominated by the one-photon process in doped nearly cubic-phase $BaTiO_3$ (see Fig. 3b). The efficient red UC radiation requires not only Yb^{3+} concentration but also level match of $^4S_{3/2} \rightarrow ^4I_{13/2}$ in Er^{3+} and $^2F_{7/2} \rightarrow ^2F_{5/2}$ in Yb^{3+} under assistance of Boltzmann distributed population within the manifold of $^4S_{3/2}$ or/and $^4I_{13/2}(Er^{3+})$ state affected by the crystal field with different symmetries for efficient EBT process. Declining tetragonality results in the centrosymmetric crystal field for high Yb^{3+}-ion to achieve the above-mentioned level matches, which may be difficult to be fulfilled with asymmetric crystal field in ferroelectric phase. It agrees with the results of XRD and of the dependence of red UC emission on structure of host materials at the same Yb^{3+} concentration.

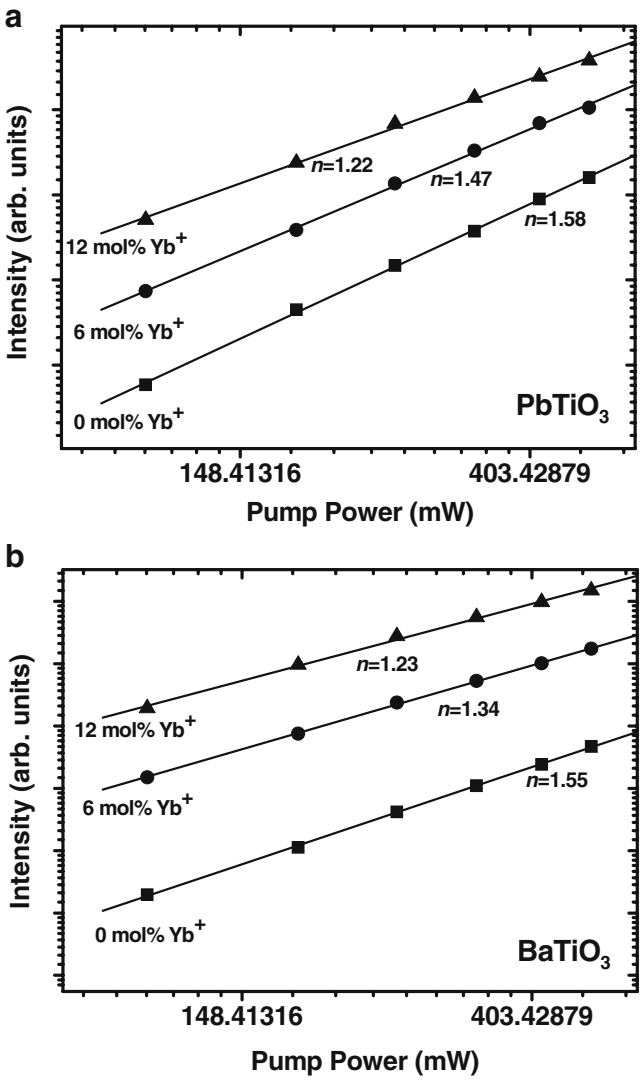

Fig. 6 Pump power dependence of the red upconversion emission of **a** $PbTiO_3$ and **b** $BaTiO_3$ doped with 6 mol% Er^{3+} ions and various concentrations of Yb^{3+} ions in a logarithmic *scale*

Conclusion

As increasing Yb^{3+} co-doped concentrations in 6 mol% Er^{3+} doped $PbTiO_3$, $BaTiO_3$, and $SrTiO_3$ polycrystalline powder samples, we have observed the room-temperature green UC emission at 550 nm being quenched by the simultaneously enhanced red UC emission at 660 nm under the 980-nm laser excitation. For codoping Yb^{3+} ions up to 6 mol% in $PbTiO_3$ and only Er^{3+} doped $PbTiO_3$ samples, which still possess relatively large tetragonality, the green UC emission is still much stronger than red one. In these cases, both the UC emissions are dominated by the two-photon process. But, as further increasing the Yb^{3+} ion concentration, the crystal structures tend to become cubic phase with enhancing red UC emission and almost diminishing in green emission. Since the pure $BaTiO_3$ crystal exhibits weaker tetragonality than $PbTiO_3$, the stronger red emission and weaker green one were expected at the lower codoped Yb^{3+} concentration in $BaTiO_3$ system than in $PbTiO_3$ one. The observed quench of green radiation accompanied with enhancement of red radiation should be due to the efficient energy back-transfer process as reported by Chen, *et al.* by raising Yb^{3+} concentration [12]. The efficient EBT process requires not only Yb^{3+} concentration but also level match of $^4S_{3/2} \rightarrow {}^4I_{13/2}$ in Er^{3+} and $^2F_{7/2} \rightarrow {}^2F_{5/2}$ in Yb^{3+} under assistance of Boltzmann distributed population within the manifold of $^4S_{3/2}$ or/and $^4I_{13/2}(Er^{3+})$ state affected by the crystal field with different symmetries. As a result, declining tetragonality results in the centrosymmetric crystal field for high Yb^{3+}-ion concentration to achieve the level match required for the EBT process that may be difficult to be fulfilled with asymmetric crystal field in the tetragonal (ferroelectric) phase.

Acknowledgments The work was supported by Grant No. NSC 96-2628-M-009-001 from the National Science Council, Taiwan.

References

1. Scheps R (1996) Prog Quantum Electron 20:271 doi:10.1016/0079-6727(95)00007-0
2. Heumann E, Bär S, Rademaker K, Huber G, Butterworth S, Dienng A, Seelert W (2006) Appl Phys Lett 88:061108 doi:10.1063/1.2172293
3. Downing E, Hesselink L, Macfarlane R et al (1996) Science 273 (5279):1185 doi:10.1126/science.273.5279.1185
4. Xu F, Lv Z, Zhang YG, Somesfalean G, Zhang ZG (2006) Appl Phys Lett 88:231109 doi:10.1063/1.2211299
5. Yi GS, Lu HC, Zhao SY, Ge Y, Yang WJ, Chen DP, Guo LH (2004) Nano Lett 4:2191 doi:10.1021/nl048680h
6. Seisenberger G, Ried MU, Endre T, Büning H, Hallek M, Bräuchle C (2001) Science 294:1929 doi:10.1126/science.1064103
7. Zeng JH, Su J, Li ZH, Yan RX, Li YD (2005) Adv Mater 17:2119 doi:10.1002/adma.200402046
8. Huber G, Heumann E, Sandrock T, Petermann K (1997) J Lumin 1:72–74 doi:10.1016/S0022-2313(96)00254-2
9. Hömmerich U, Nyein E, Trivedi SB (2005) J Lumin 113:100 doi:10.1016/j.jlumin.2004.09.111
10. Chen GY, Zhang YG, Somesfalean G, Zhang ZG, Sun Q, Wang FP (2006) Appl Phys Lett 89:163105 doi:10.1063/1.2363146
11. Chen GY, Liu Y, Zhang YG, Somesfalean G, Zhang ZG, Sun Q, Wang FP (2007) Appl Phys Lett 91:133103 doi:10.1063/1.2787893
12. Chen GY, Somesfalean G, Liu Y, Zhang Z, Sun Q, Wang FP (2007) Phys Rev B 75:195204 doi:10.1103/PhysRevB.75.195204
13. Muller KA, Burkard H (1979) Phys Rev B 19:3593 doi:10.1103/PhysRevB.19.3593
14. Chang NC, Gruber JB, Leavitt RP, Morrison CA (1982) J Chem Phys 76:3877 doi:10.1063/1.443530
15. Gruber JB, Sardar DK, Russell CC, Yow RM, Zandi B, Kokanyan EP (2003) J Appl Phys 94:7128
16. Gruber JB, Yow RM, Nijjar AS, Russell CC, Sardar DK, Zandi B et al (2006) J Appl Phys 100:043108
17. Kuo SY, Chen CS, Tseng TY, Chang SC, Hsieh WF (2002) J Appl Phys 92:1868
18. Kuo SY, Li CT, Hsieh WF (2002) Appl Phys Lett 81:3019 doi:10.1063/1.1513660
19. Chamarro MA, Cases R (1988) J Lumin 42:267 doi:10.1016/0022-2313(88)90054-3
20. Pollnau M, Gamelin DR, Lüthi SR, Güdel HU, Hehlen MP (2000) Phys Rev B 61:3337 doi:10.1103/PhysRevB.61.3337